Basin-scale cyclostratigraphy of the Green River Formation, Wyoming

W. Aswasereelert[1,2,†], S.R. Meyers[1], A.R. Carroll[1], S.E. Peters[1], M.E. Smith[3], and K.L. Feigl[1]
[1]*Department of Geoscience, University of Wisconsin, 1215 West Dayton Street, Madison, Wisconsin 53706, USA*
[2]*Department of Earth Sciences, Faculty of Science, Kasetsart University, 50 Phahon Yothin Road, Chatuchak, Bangkok 10900, Thailand*
[3]*Department of Geology, Sonoma State University, 1801 East Cotati Avenue, Rohnert Park, California 94928, USA*

ABSTRACT

The fluviolacustrine Wilkins Peak Member of the Eocene Green River Formation preserves repetitive sedimentary facies that have been interpreted as an orbitally induced climate signal. However, previous quantitative studies of cyclicity in this member have used oil-yield data derived from single locations. Here, macrostratigraphy is used to quantitatively describe the spatiotemporal patterns of three different lithofacies associations from 8 to 12 localities that span much of the basin. Macrostratigraphic time series demonstrate that there is a reciprocal basin-scale relationship between carbonate-rich lacustrine facies and siliciclastic-rich alluvial facies. Spectral analyses identify statistically significant periods (≥90% confidence level) in basin-scale sedimentation that are consistent with Milankovitch-predicted orbital periodicities, with a particularly strong ~100 k.y. cycle expressed in all lithofacies associations. Numerous non-Milankovitch periods are also recognized, indicating complex depositional responses to orbital forcing, autocyclic controls on sedimentation, or harmonic artifacts. Although fluctuations in Lake Gosiute water level did affect basin-scale patterns of sedimentation, they are not directly related to the 100 k.y. short-eccentricity cycle, as previously supposed. Instead, 100 k.y. cycles are principally recorded by the recurrence of alluvial environments, which exerted a dominant control on basin-scale patterns of sedimentation generally. Thus, the hydrologic controls on lake level that have been classically linked to short-eccentricity actually occurred at finer temporal scales (<100 k.y.). Understanding the complex links between orbital forcing and sedimentation in the Wilkins Peak Member is facilitated by analysis of time series that reflect spatial as well as temporal variability in stratigraphic data. Macrostratigraphy is, therefore, promising as an analytical tool for basin-scale cyclostratigraphy.

INTRODUCTION

Astrochronology has become an important tool for advancing the completeness and resolution of the geologic time scale (Hinnov and Ogg, 2007). The principal technique, called orbital tuning, is a method of aligning a stratigraphic succession thought to express precession, tilt, and/or eccentricity periods with a target orbital signal. This allows finely resolved numerical ages to be assigned to sedimentary successions. However, interpreting results based on orbital tuning can lead to circular reasoning, because the presence of an orbital signal is commonly assumed before it is tested. Furthermore, the outcome depends on choosing an appropriate target curve and/or a frequency for tuning. As a result, astrochronology may provide multiple unconstrained orbital interpretations for a given stratigraphy (e.g., Meyers et al., 2001; Prokoph et al., 2001; Meyers and Sageman, 2007).

Orbital tuning and other methods of calibrating astrochronology commonly embed assumptions that depositional rates are constant through time, that lateral facies changes are negligible, and/or that the preserved record is essentially complete on Milankovitch time scales. Such conditions are likely to be quite rare. The fact that orbital signals are nonetheless commonly recognized is perhaps a testament to their inherent strength, which allows them to rise above a certain level of stratigraphic noise. However, the way in which complex sedimentologic processes may have altered the relationship between the original climate forcing and the observed stratigraphic signal is little known. Drawing an analogy to the processes that selectively preserve fossil evidence of past life, the dynamics of sedimentary systems might impose a taphonomic filter on apparent modes of past climatic forcing. The concept has seldom been addressed, although modeling studies illuminate some plausible impacts (e.g., Goreau, 1980; Pestiaux and Berger, 1984; Ripepe and Fischer, 1991; Meyers et al., 2001; Laurin et al., 2005; Meyers et al., 2008; Jerolmack and Paola, 2010).

The Wilkins Peak Member of the Eocene Green River Formation in Wyoming presents an excellent opportunity to test such questions, due to its combination of variable sedimentary deposits and readily accessible outcrops and drill cores. Lake deposits of the Green River Formation have long been believed to express Milankovitch-band cyclicity (e.g., Bradley, 1929; Fischer and Roberts, 1991; Roehler, 1993), and the Wilkins Peak Member is marked by especially vivid vertical and lateral lithologic contrasts (Smoot, 1983; Pietras and Carroll, 2006). Most importantly, radioisotopic dating of interbedded tuffs has established a robust and independent set of ages for the Wilkins Peak Member with uncertainties on the order of 100 k.y. (Smith et al., 2010). This age framework places the Wilkins Peak Member among the best-dated pre-Quaternary stratigraphic intervals in the world, reducing the need for orbital tuning and its associated issues.

Wilkins Peak Member strata have been interpreted to preserve a record of orbital climate forcing based on spectral analyses of organic matter enrichment as measured by Fisher assay (Machlus et al., 2008; Meyers, 2008). Although the results differed in detail, both studies reported power spectra dominated by long and short eccentricity. Both also reported multiple sub–100 k.y. spectral peaks at substantially lower power, some of which were interpreted to record obliquity and precession cycles. At face value, such results are puzzling, because the influence of eccentricity variability on climate must primarily result from the modulation of precession (Laskar et al., 2004). The observation of high eccentricity–band power concomitant with lower precession–band power suggests the presence of a nonlinear climate and/or depositional system response to orbital insolation (e.g., Ripepe and Fischer, 1991), whereby spectral

†E-mail: wasinee@geology.wisc.edu

GSA Bulletin; January/February 2013; v. 125; no. 1/2; p. 216–228; doi: 10.1130/B30541.1; 10 figures; 1 table; Data Repository item 2012243.

power is transferred from carrier frequency (precession) to its modulator (eccentricity).

The present study examines the Wilkins Peak sedimentary patterns in greater depth, through use of a quantitative technique called macrostratigraphy (Peters, 2006; Hannisdal and Peters, 2010). It allows the quantification of spatiotemporal patterns in the rock record, which can be expressed as the temporal ranges of gap-bound rock packages. In contrast to previous studies that were based on single localities, macrostratigraphy is used to integrate stratigraphic patterns compiled separately at multiple localities across the basin. It therefore incorporates spatial variability directly into the quantitative stratigraphic analyses. Macrostratigraphy also allows the derivation of facies-specific time series. This approach thus provides new insight into the influence of temporally distinct sedimentary processes on the derived stratigraphic expression of the orbital signals. The present study is the first to employ macrostratigraphy at the scale of an individual nonmarine basin.

The goal of this study is to introduce a novel integration of macrostratigraphy and cyclostratigraphy that can be applied to quantitatively analyze sedimentary patterns in any stratigraphic record. This study also provides a new data set for future numerical analysis of the sedimentology and stratigraphy of the Wilkins Peak Member. Finally, a new interpretation of depositional controls on repetitive stratigraphic successions of the Wilkins Peak Member is proposed.

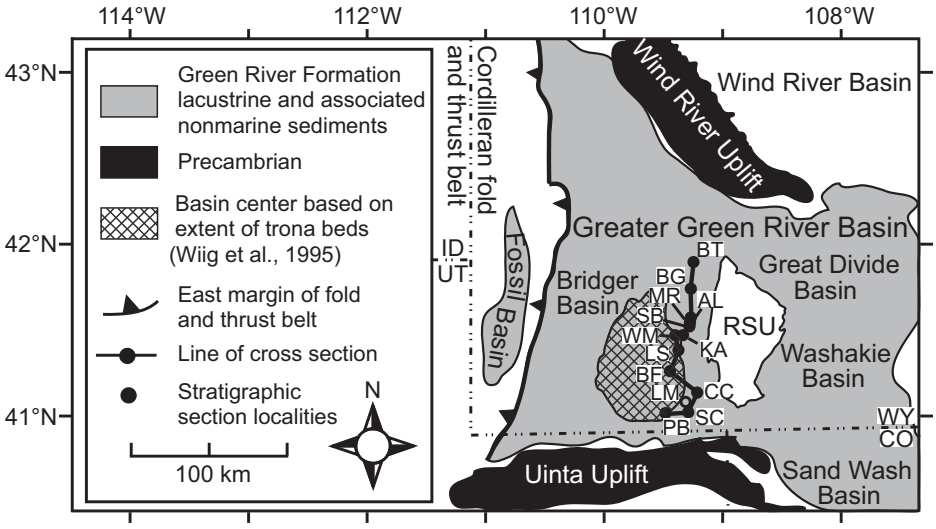

Figure 1. Location of Eocene lacustrine basins and associated Precambrian-cored uplifts in the northern Rocky Mountains. BT—Boar's Tusk outcrop, BG—Breathing Gulch outcrop, AL—Apache Lane outcrop, MR—Microwave Reflector outcrop, SB—Stagecoach Boulevard outcrop, KA—Kanda outcrop, WM—White Mountain #1 core, LS—Lauder Slide outcrop, BF—U.S. ERDA/LERC 1 Blacks Fork core, CC—Currant Creek outcrop, SC—Spring Creek outcrop, PB—Pipeline Bridge outcrop, LM—Little Mountain, RSU—Rock Springs Uplift, CO—Colorado, ID—Idaho, UT—Utah, WY—Wyoming. Figure is modified from Smith et al. (2003, 2008). See Table DR1 for coordinates of all stratigraphic sections (see text footnote 1).

GEOLOGIC SETTING

The Wilkins Peak Member of the Green River Formation was deposited in Eocene Lake Gosiute during an underfilled phase of the Bridger Basin in southwestern Wyoming (Carroll and Bohacs, 1999; Fig. 1). The Bridger Basin is bounded on the west by the Cordilleran fold-and-thrust belt, and on the south and north by basement-cored foreland uplifts. The Rock Springs Uplift bounds the Bridger Basin to the east and exposes a north-south–trending series of Wilkins Peak Member outcrops. The 10 outcrops and 2 cores used in this study are mostly on the eastern flank of the Wilkins Peak depocenter. This transect does not extend directly into the Wilkins Peak Member depocenter, but the availability of continuous exposure permits exceptionally detailed stratigraphic correlations to be carried across much of the basin. Due to the low gradient of the basin floor, the large magnitude of lake-level changes, and the high frequency of those changes, the transect does capture a wide range of lacustrine and fluvial sedimentary facies. The principal limitation of this transect is that it excludes the thickest-bedded evaporite deposits. Because they lack appreciable organic enrichment, those deposits are also not clearly recorded in the Fischer assay data employed in previous cyclostratigraphic studies (Machlus et al., 2008; Meyers, 2008).

Deposition of the Wilkins Peak Member occurred between ca. 51.56 and 49.89 Ma, coinciding with the peak of the early Eocene climatic optimum (Zachos et al., 2001; Smith et al., 2008, 2010). As such, it is one of only a few records of Eocene warm climate variability with the potential for age resolution on the scale of tens of thousands of years (Zachos et al., 1994; Sloan and Rea, 1996). Leaf fossils collected at Little Mountain (Fig. 1) from sites spanning the boundary between the Wilkins Peak and overlying Laney Members indicate warm subtropical conditions, with a mean annual precipitation of ~80 cm/yr (Wilf, 2000). Bedded evaporite intervals stratigraphically lower in the Wilkins Peak Member suggest either a long-term transition toward wetter conditions (Wilf, 2000), or the existence of high-frequency (and high-amplitude) climatic fluctuations during deposition of the unit (Smith et al., 2008).

Although commonly characterized as entirely lacustrine, the Wilkins Peak Member actually consists of two distinctly different lithofacies assemblages: carbonate- and evaporite-rich lake deposits, and siliciclastic alluvial deposits. Lacustrine lithologies include tan to olive micrite and carbonate siltstone, kerogen-rich laminated micrite (oil shale), bedded evaporite, and minor carbonate-cemented siliciclastic sandstone. Carbonate mineralogies include both calcite and dolomite. These lithologies are organized into at least 126 repetitive vertical successions (cycles), ranging from 0.14 m to nearly 6 m thick, which are interpreted to record discrete expansions and subsequent contractions of Lake Gosiute (Pietras and Carroll, 2006). Lake expansions are often marked by oil shale beds, and thus are associated with increased Fischer assay oil yields (Roehler, 1993). Desiccation cracks, scours, and pedogenically brecciated facies are common and may denote lacunae of unknown duration (Smoot, 1983; Pietras and Carroll, 2006). The preservation of lake cycles is not uniform across the basin; the number of recognizable cycles approximately increases by a factor of three from the northern basin margin to the basin center (a distance of ~50 km; Pietras et al., 2003; Pietras and Carroll, 2006). Many of these cycles likely reflect Milankovitch forcing of climate, but some clearly do not. Calculation of an average apparent cycle duration using $^{40}Ar/^{39}Ar$ tuff ages (Pietras et al., 2003) and spectral analysis (Machlus et al., 2008) demonstrated the existence of subprecessional cycles in the Wilkins

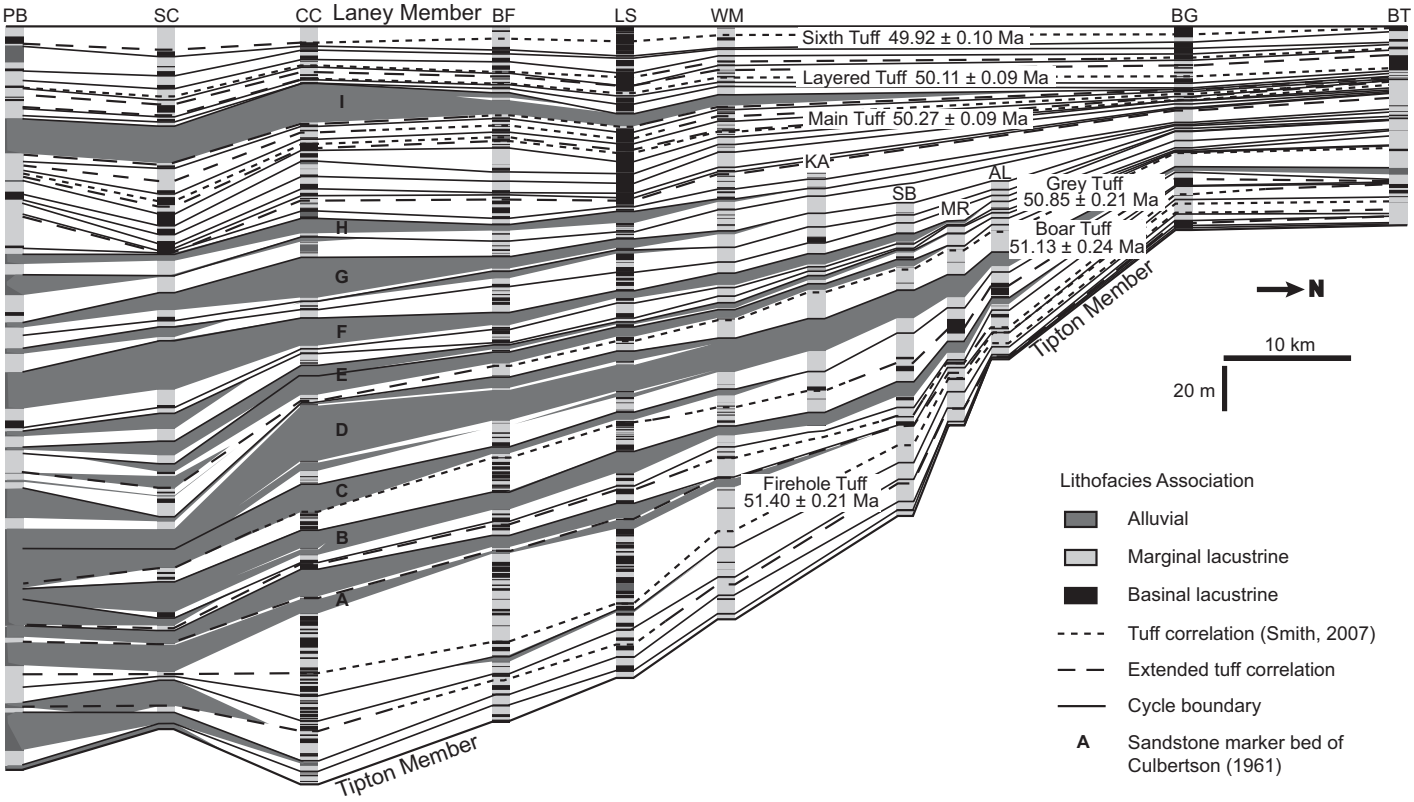

Figure 2. Cross section of the Wilkins Peak Member of the Green River Formation showing distribution of its three distinct facies associations: alluvial, marginal lacustrine, and basinal lacustrine (adapted from Pietras and Carroll, 2006; Smith, 2007). $^{40}Ar/^{39}Ar$ ages of Sixth, Layered, Main, Grey, Boar, and Firehole Tuffs are from Smith et al. (2010). The extended tuff correlation is based on further investigation of gamma-ray signature and stratigraphic correlation. Cycle boundaries are defined by lacustrine flooding surfaces that can be traced along the transect. All 15 tuffs and 34 cycle boundaries, including the top and the bottom of the Wilkins Peak Member, were used to establish time-equivalent surfaces (TES). See Table DR2 and DR3 for cumulative thickness versus each facies association and cumulative thickness versus TES, respectively (see text footnote 1). PB—see Fig. 1 for stratigraphic section definitions.

Peak Member. However, the causes of subprecessional fluctuations of Lake Gosiute remain unknown.

Wilkins Peak lacustrine strata are punctuated by up to nine composite alluvial bed sets, composed of silty mudstone to medium-grained sandstone (marker beds A–I of Culbertson, 1961; Pietras and Carroll, 2006). These alluvial intervals represent up to ~48% of the thickness of the Wilkins Peak Member and are most prominent in the southern Bridger Basin (Fig. 2). Lenticular sandstone beds associated with basal scours and trough cross-bedding are interpreted as fluvial deposits (Pietras and Carroll, 2006). Climbing ripples and planar-parallel lamination are common to ubiquitous, implying rapid deposition from sediment-laden unidirectional flows. Bird and other vertebrate tracks, insect burrows, root casts, and incipient paleosols attest to at least occasional subaerial exposure (Pietras and Carroll, 2006), and exclude a purely lacustrine origin for the siliciclastic facies. Lacustrine carbonate facies do occasionally occur as meter-scale interbeds however, consistent with a model of fluvial deposition on a low-relief lake plain. The alluvial intervals are readily correlatable across distances of tens of kilometers and appear conformable with major oil shale beds and other lacustrine strata.

METHODS

Facies Associations

The Wilkins Peak lithology is classified into three distinct facies associations that denote lake water depth during deposition: alluvial, marginal lacustrine, and basinal lacustrine facies associations (Fig. 2, Tables DR1 and DR2[1]). The alluvial facies association represents a wide range of fluvial channel deposits, represented by arkosic sandstone-siltstone-mudstone bed sets. The marginal lacustrine facies association was deposited in shallow-water environments undergoing both subaqueous deposition, with dominant wave transportation, and subaerial modification. The basinal lacustrine facies association, including kerogen-rich micrite (oil shale) and bedded evaporite, represents deep lacustrine environments. The oil shale facies was deposited in a calm and low-oxygen environment, which allowed concentration and preservation of organic matter. Close to the basin center, oil shale is commonly intercalated with bedded evaporite (Pietras and Carroll, 2006; Smith, 2007), which is interpreted as having been deposited subaqueously on the lake floor (Bradley and Eugster, 1969).

Chronostratigraphic Correlation

A basin-scale cross section is compiled from two separate cross sections in the northern and the southern parts of the Bridger Basin, based on

[1]GSA Data Repository item 2012243, stratigraphic information including locations, and key surfaces versus thickness and time, is available at http://www.geosociety.org/pubs/ft2012.htm or by request to editing@geosociety.org.

decimeter-scale lithologic description of 12 outcrop and core sections (Fig. 2; Table DR 1 (see footnote 1); Pietras and Carroll, 2006; Smith, 2007). Lateral correlation among these sections is considerably aided by 15 tuff horizons, 9 composite bed sets of the alluvial association (A–I), and 34 major lake cycles. The $^{40}Ar/^{39}Ar$ ages of six tuffs within the Wilkins Peak interval, including the Sixth, Layered, Main, Grey, Boar, and Firehole Tuffs, have been recently recalculated to account for the new 28.201 Ma value for the Fish Canyon standard and to eliminate altered samples from weighted mean age calculations (Kuiper et al., 2008; Smith et al., 2010). The nine sandstone-siltstone-mudstone marker beds (A–I; Culbertson, 1961) are up to 25 m thick and can be traced across much of the basin, especially in the southern part. Expansion-contraction cycles of Eocene Lake Gosiute represented by the repetitive carbonate-rich facies successions of the Wilkins Peak Member are bounded by widely traceable lacustrine flooding surfaces (Bohacs, 1998). The 34 major lake cycles are defined by the flooding surfaces that can be traced across the basin.

Thickness-To-Time Transformation

The six dated tuffs within the Wilkins Peak interval, including the Sixth, Layered, Main, Grey, Boar, and Firehole Tuffs, yield weighted mean ages (±2σ analytical uncertainties) of 49.92 ± 0.10 Ma, 50.11 ± 0.09 Ma, 50.27 ± 0.09 Ma, 50.85 ± 0.21 Ma, 51.13 ± 0.24 Ma, and 51.40 ± 0.21 Ma, respectively (Fig. 2; Smith et al., 2010). Based on the nominal tuff ages, age models for the eight stratigraphic sections that extend from the base to the top of the Wilkins Peak Member were calculated using least-squares fits of second-order polynomials (quadratic model), which provide exceptional fits to the $^{40}Ar/^{39}Ar$ ages ($r^2 > 0.99$), compared to linear and exponential age models (Fig. 3). The primary assumption involved in the application of this model is that long-term secular changes in sedimentation rate can be modeled as a smooth, slowly varying function, providing a reliable reconstruction of the time-depth relationship within ~0.06 m.y. (the maximum root mean square misfit of the models across the eight study sites). Importantly, the quadratic model avoids an assumption of constant sedimentation rate. Higher-frequency sedimentation rate variability could still be present, but is not resolvable with the available radioisotopic data. As discussed in detail later herein, the upper and the lower contacts of the Wilkins Peak Member, the six dated tuffs plus nine other tuffs, and the 34 major lake cycle boundaries were all used to establish time-equivalent surfaces (Fig. 2, Table DR3 (see footnote 1).

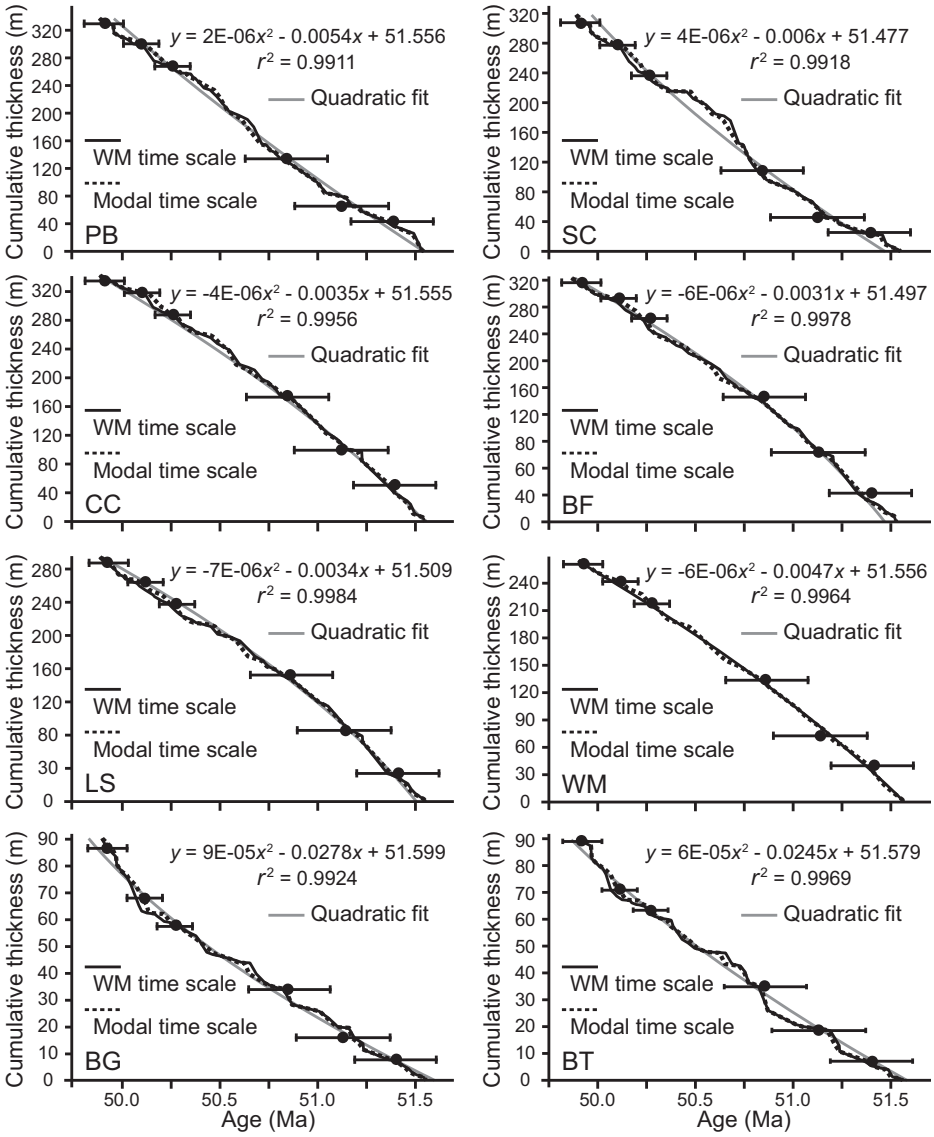

Figure 3. Second-order polynomial age models for the eight stratigraphic sections that extend from the base to the top of the Wilkins Peak Member (PB, SC, CC, BF, LS, WM, BG, and BT) based on $^{40}Ar/^{39}Ar$ ages of the Sixth, Layered, Main, Grey, Boar, and Firehole Tuffs (see Figs. 1 and 2 for locations of the stratigraphic sections and the tuffs). The ages of 51 time-equivalent surfaces based on the WM time scale and the modal time scale are also plotted for comparison with the $^{40}Ar/^{39}Ar$ ages. The horizontal bars indicate ±2σ analytical uncertainties of the $^{40}Ar/^{39}Ar$ ages (Smith et al., 2010).

To examine the reliability and sensitivity of the analysis to implicit assumptions associated with the time models, two depth-derived time scales were calculated: the "WM time scale" and the "modal time scale." The WM time scale is based on the ages of time-equivalent surfaces at the WM site, and is motivated by the fact that this is one of only two stratigraphic sections (WM and BG) where all six dated tuffs are unambiguously identified (Smith, 2007; Figs. 2 and 3). Between the two, only the WM section preserves all Wilkins Peak lithofacies (Pietras and Carroll, 2006), and it is much closer to the basin center, so it is a more appropriate representative for the Wilkins Peak age model. The ages of the time-equivalent surfaces at the 11 other stratigraphic sections were rescaled to match those of the WM section.

The "modal time scale" was derived from the ages of time-equivalent surfaces at all eight localities (Figs. 2 and 3). Kernel density estimates of the ages of each time-equivalent surface were evaluated to investigate their distribution and to find the most appropriate

central tendency that best represented those ages (Fig. 4; Silverman, 1982). The Gaussian kernel function computes a probability density estimate evaluated at 100 equally spaced points that cover the range of those ages. As shown in Figure 4, the kernel density distribution represents the modeled age distribution better than the classic Gaussian distribution, especially when the ages are not unimodal or somewhat skewed. We used the mode of the ages based on the kernel distribution of each time-equivalent surface to establish the depth-derived time scale at all sites, and it also provides an estimate of the age uncertainty. This approach is an adaptation of the depth-derived age model technique of Huybers and Wunsch (2004), which utilizes mean ages.

Both time scales were used independently to transform stratigraphic thickness into geologic time, by assuming a constant rate of sedimentation between successive time-equivalent surfaces (Figs. 5A and 5B). Finally, the original lithostratigraphic cross section was transformed to show the distribution of the Wilkins Peak facies in a chronostratigraphic framework that essentially constitutes a Wheeler diagram (Figs. 6 and 7; Tables DR2 and DR3 (see footnote one); Wheeler, 1958). However, the distribution and duration of possible lacunae at each location remain a source of uncertainty.

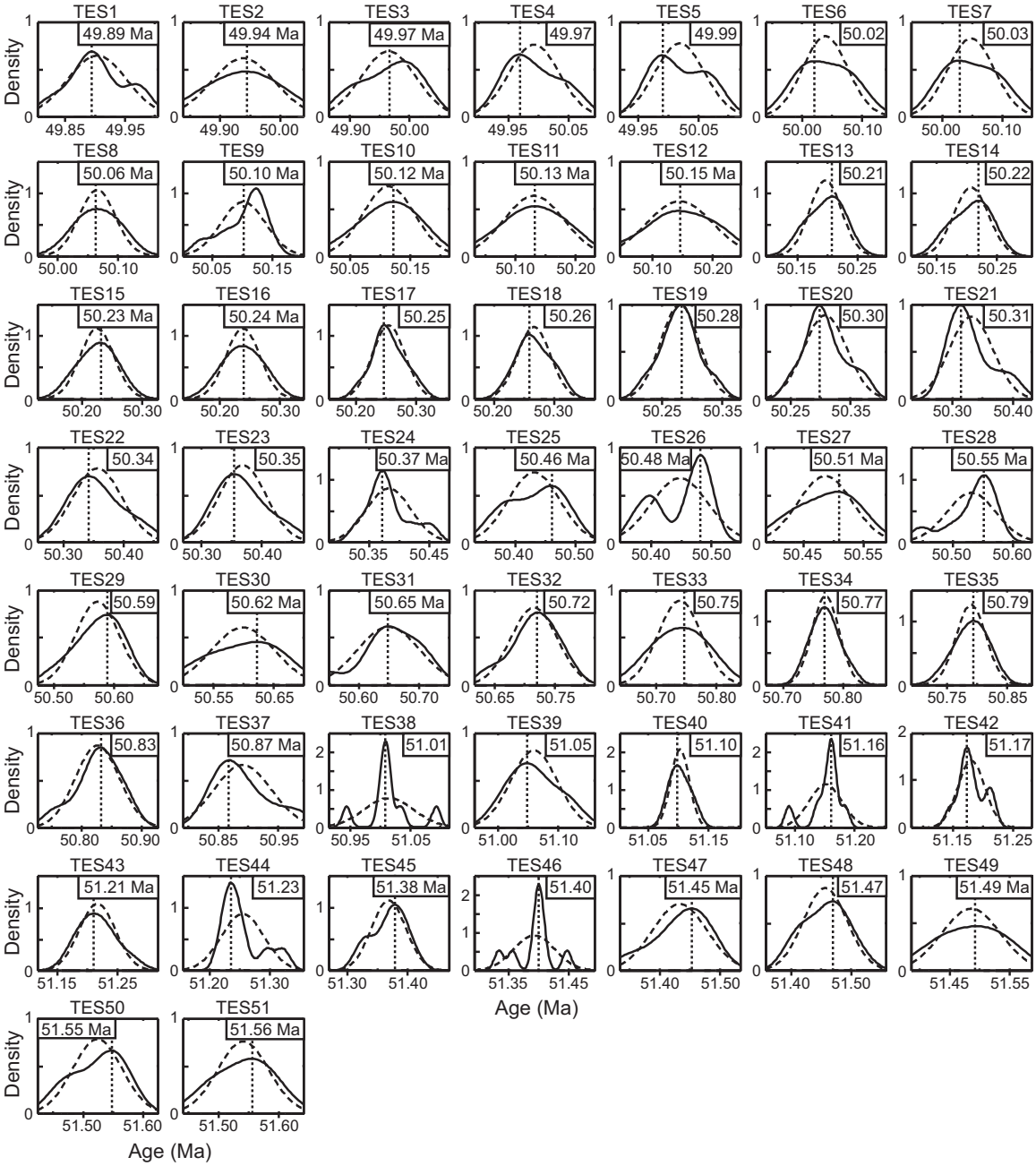

Figure 4. Gaussian (dashed line) and kernel density (solid line) distributions of the ages of each time-equivalent surface (TES) derived from the eight polynomial equations shown in Figure 3. Vertical dotted lines indicate ages used for the modal time scale (Fig. 3). All *x*-axes are scaled identically.

Macrostratigraphic Analysis

We used macrostratigraphy (Peters, 2006) to quantify spatiotemporal patterns of the repetitive successions of the Wilkins Peak Member. Each continuous facies association in each stratigraphic section constitutes a rock package (or "facies package") bounded by temporal gaps that are defined by rock packages of different facies associations. In addition to the three facies associations, a total lacustrine facies association that is an integration of the marginal and the basinal lacustrine facies associations was included in the analysis to test the reliability of the macrostratigraphic analysis. Spectra of alluvial and total lacustrine macrostratigraphic time series should be essentially identical, as they are expected to be reciprocal to one another.

Following application of the time scales (both WM and modal) to all 12 stratigraphic sections, we identified the temporal gaps that are shorter than the smallest resolvable gap (0.4 k.y.). The facies packages that were separated by an interval shorter than the smallest resolvable gap were considered to be one continuous package. Then, the 12 stratigraphic sections were uniformly resampled at a 0.4 k.y. interval, to measure the spatiotemporal continuity of each rock package (Fig. 5C). The 0.4 k.y. interval was chosen for both the sampling interval and the smallest resolvable gap because the detailed

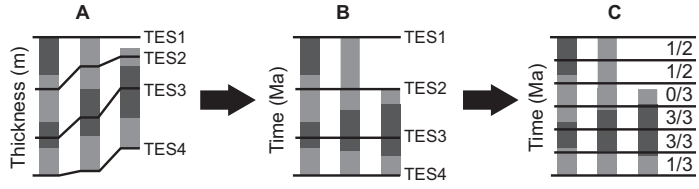

Figure 5. Diagram describing the thickness-to-time transformation and macrostratigraphic analysis. (A) A schematic cross section consisting of two facies represented by dark and light gray in combination with four time-equivalent surfaces (TES). (B) A chronostratigraphic cross section after thickness-to-time transformation. Note that the distribution and duration of possible lacunae remain unknown. (C) A resampled cross section in combination with stratigraphic abundance of the dark-gray facies in each temporal bin. Numerators are number of the dark-gray facies in each temporal bin. Denominators are number of stratigraphic sections in each temporal bin.

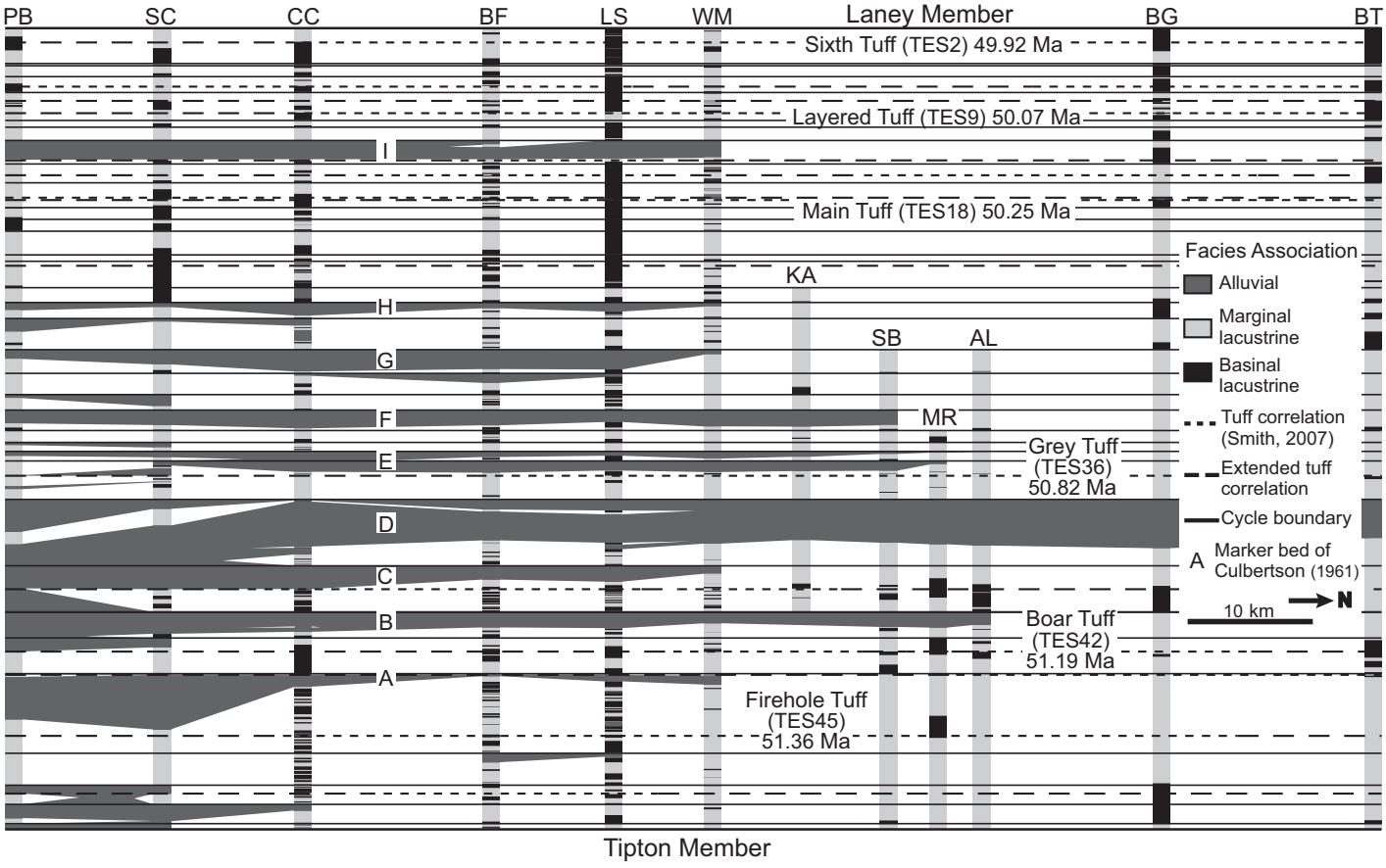

Figure 6. Chronostratigraphic cross section of the Wilkins Peak Member based on the WM time scale. Note that the Wilkins Peak interval spans approximately from 49.89 to 51.56 Ma. The vertical and horizontal axes represent time and position within the basin, respectively. See Table DR2 for the WM time scale versus each facies association, and Table DR3 for the WM time scale versus time-equivalent surface (see text footnote 1). PB—see Fig. 1 for stratigraphic section definitions.

cross section has a resolution of 10 cm, which is equivalent to a nominal temporal resolution of 0.3–0.5 k.y. (Machlus et al., 2008). The number of occurrences of each facies package in each temporal bin was then summed across the basin. Stratigraphic abundance, the ratio of the number of occurrences of each facies package to the number of stratigraphic sections in each temporal bin, was then calculated (Fig. 5C). This approach distills the stratigraphic architecture into a macrostratigraphic time series for each facies association (Fig. 8). Quantitative changes in this ratio correspond to expansion (large stratigraphic abundance) and contraction (small stratigraphic abundance) in the area of deposition of each facies association. Consequently, the macrostratigraphic time series reflect both the spatial extent and the temporal continuity of each facies association. As a result, they should capture temporal ranges of forcing mechanisms that controlled the stratigraphic pattern of the Wilkins Peak Member.

Cyclostratigraphic Analysis via Multitaper Method Spectral Analysis

We used multitaper method spectral analysis (MTM) of the macrostratigraphic time series to estimate power spectra, allowing a quantitative assessment of the Wilkins Peak cyclicity (Fig. 9; Thomson, 1982). The MTM technique also includes a harmonic F variance-ratio test (F-test) for the presence of periodic components (phase-coherent sinusoids). The F-test is independent of amplitude, and thus the statistical significance of both weak and strong periodic signals can be evaluated. This approach is particularly useful in stratigraphic data series, which are generally noisy, as is the case for the Wilkins Peak time series (Meyers, 2008; Machlus et al., 2008). The analysis was conducted using five 3π prolate tapers, following the removal of a linear trend from the data (Thomson, 1982). The present study focuses on cycles with periods longer than 10 k.y. that have previously been hypothesized to record orbital forcing in the Wilkins Peak Member (Fischer and Roberts, 1991; Roehler, 1993; Machlus et al., 2008; Meyers, 2008), although the 0.4 k.y. sampling interval allows for assessment of frequencies as high as 1.25 cycles/k.y., corresponding to a period of 0.8 k.y.

RESULTS

Age Model

The quadratic age models for the eight stratigraphic sections that span the entire Wilkins Peak Member provide evidence that net average sediment accumulation rates varied both temporally and geographically within the Bridger Basin (Fig. 3). The pattern of these variations, as expressed at individual localities, is broadly consistent with the proximity to the Wilkins Peak depocenter to the west and the Uinta Uplift to the south (Fig. 1). Four of

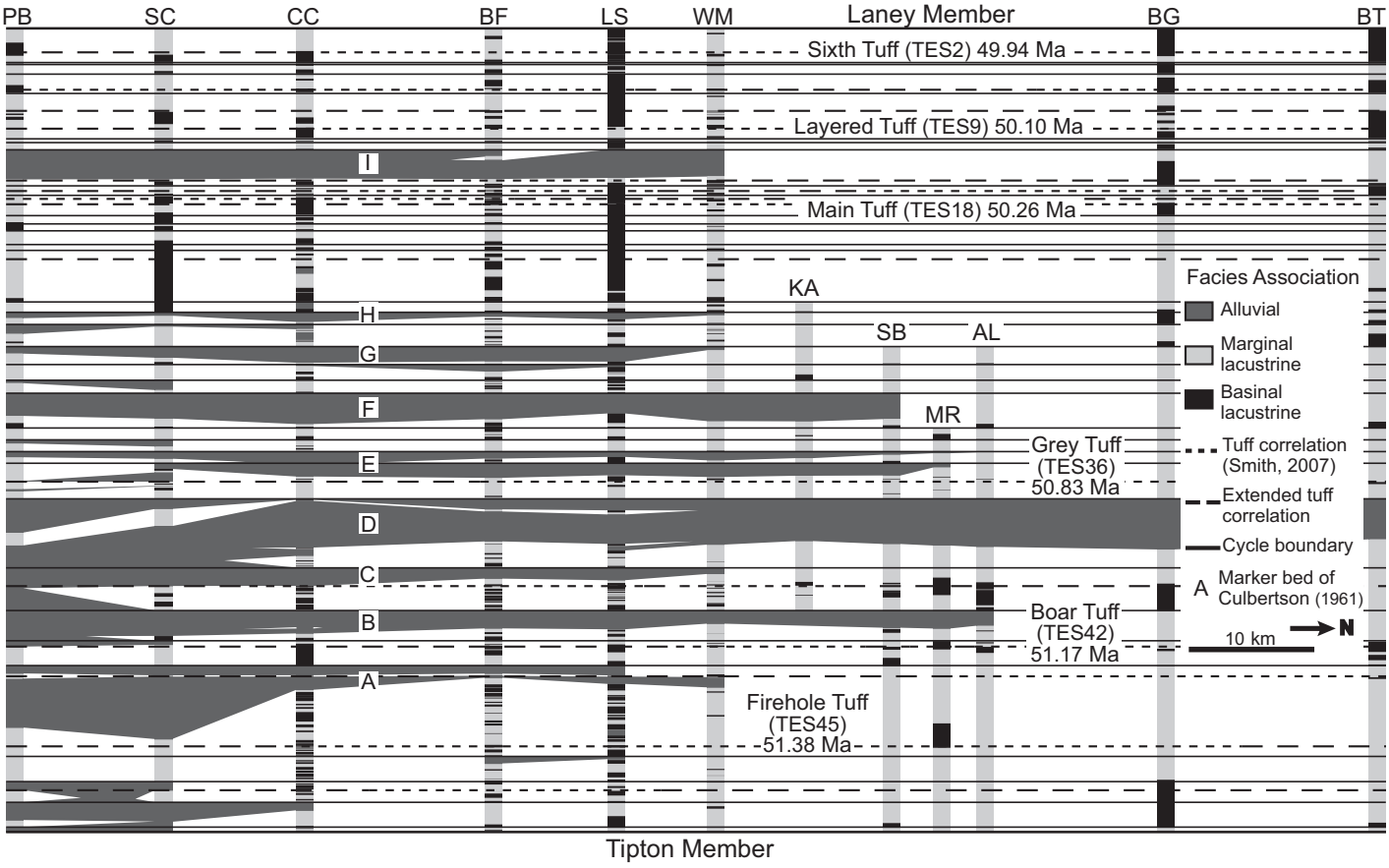

Figure 7. Chronostratigraphic cross section of the Wilkins Peak Member based on the modal time scale. Note that the Wilkins Peak interval spans approximately from 49.89 to 51.56 Ma. The vertical and horizontal axes represent time and position within the basin, respectively. See Table DR2 for the modal time scale versus each facies association, and Table DR3 for the modal time scale versus time-equivalent surface (see text footnote 1). PB—see Fig. 1 for stratigraphic section definitions.

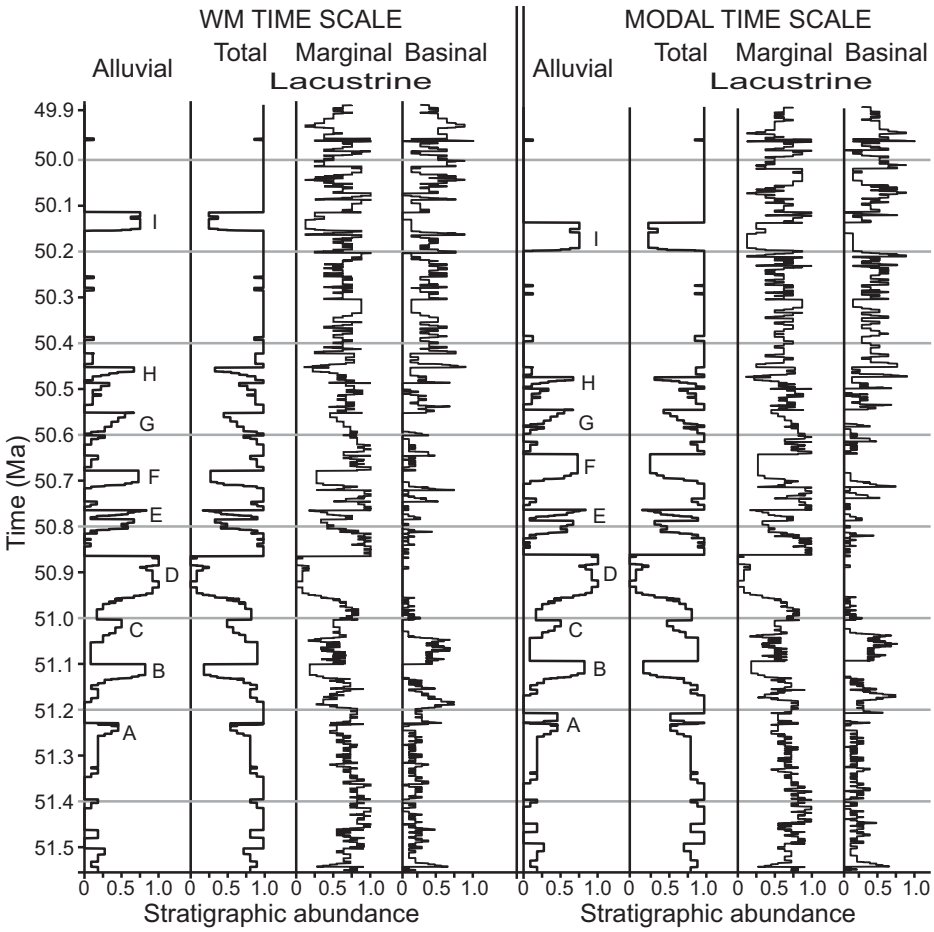

Figure 8. Macrostratigraphic time series of each Wilkins Peak facies association following application of the WM time scale (left) and the modal time scale (right). A–I represent the alluvial marker beds of Culbertson (1961).

the localities (CC, LS, BF, and WM) share a history of diminishing net accumulation rate with decreasing age, whereas the other four sections (PB, SC, BG, and BT) exhibit an apparent acceleration of net accumulation rate (Fig. 3). Also, the rate generally increases to the south. For example, the net accumulation rate between the Boar Tuff and the Firehole Tuff varies from 224 m/m.y. at WM to 44 m/m.y. at BT, while the rate between the Sixth Tuff and the Layered Tuff varies from 163 m/m.y. to 67 m/m.y. across the basin. This history is consistent with the observation of greater stratal thicknesses in the southern part of the basin and a more uniform accumulation rate late in the history of Wilkins Peak Member deposition (Fig. 2). When the time-depth relationships based on the WM and the modal time scales are compared, it is found that the ages of the Wilkins Peak strata show greater discrepancy from each other in the upper portion of the stratigraphy, approximately above the Grey Tuff (Fig. 3).

Macrostratigraphic Time Series

Macrostratigraphic time series based on the WM and modal time scales are similar to each other in the lower half of the Wilkins Peak Member, except for the interval from the upper A bed to the lower B bed (Fig. 8). On the contrary, they demonstrate greater discrepancy in the upper half (above the E bed), indicating that the results are sensitive to the time scale used to reconstruct the time-depth relationship. For both time scales, the nine alluvial marker beds (A–I) dominate the alluvial time series, and align with corresponding but opposite signals expressed by the total lacustrine facies association. Although this strongly reciprocal relationship can be visually recognized from the Wilkins Peak cross sections (Figs. 2, 6, and 7), it is directly quantified via the macrostratigraphic time series. The marginal and basinal lacustrine associations individually exhibit higher-frequency variability, quantified using power spectral analysis (see "Multitaper Method Power Spectra" below), than either the alluvial facies association or the combined lacustrine association. The lack of high-frequency variation in the combined lacustrine association suggests that its constituent parts are consistently out phase with each other, as would be expected if the lake-level changes were (nearly) synchronous across the basin.

Multitaper Method Power Spectra

Spectral analysis of the stratigraphic abundance of each facies association identified numerous periods that are significant at the 90% harmonic F-test confidence level (Fig. 9). The periods range from 10 to 1000 k.y., and many of them are consistent with the predicted orbital frequencies (Table 1; Laskar et al., 2004, 2011). Although a detailed comparison of the WM and modal time-scale spectra reveals some sensitivity to the proscribed thickness-to-time transformation, a remarkably consistent feature of all analyses is the concentration of power at a frequency of ~1/100 k.y. (Fig. 9). The WM time scale alluvial and lacustrine spectral results illustrate exceptionally strong periodic variability at ~1/100 k.y.; the highest values of the harmonic F statistic occur at this frequency, exceeding the 99% confidence level, and the power spectra also exhibit plateaus that are diagnostic of a robust periodicity (Thomson, 1990).

The presence of a well-defined ~1/100 k.y. peak with high power in all of the facies association spectra (most of which also achieve F statistic confidence levels exceeding 90%), and the fact that the WM time scale brings this 100 k.y. cycle into such strong phase-coherence provide substantial evidence in favor of the WM time scale (Fig. 9; Table 1). This follows similar statistical reasoning as employed in "minimal tuning" (Muller and MacDonald, 2000). That is, if the process of tuning to one orbital component (e.g., obliquity) yields enhanced phase-coherence in another component (e.g., eccentricity), it is difficult to reconcile such sharpening of spectral features as a statistical coincidence, lending support to the tuning. The 100 k.y. cycle that is expressed in the Wilkins Peak macrostratigraphic data is consistent with previously hypothesized short-eccentricity variability; however, this result is particularly remarkable considering that orbital tuning was not applied to the macrostratigraphic time series. Importantly, the 100 k.y. cycle demarcates the timing of almost all alluvial strata that are identified in the basin (Fig. 8), indicating that this periodicity is strongly tied to the alternation of lacustrine and alluvial facies associations.

Frequencies higher than 1/100 k.y. contain less power and are more sensitive to the choice of the WM versus the modal time scale (Fig. 9). This

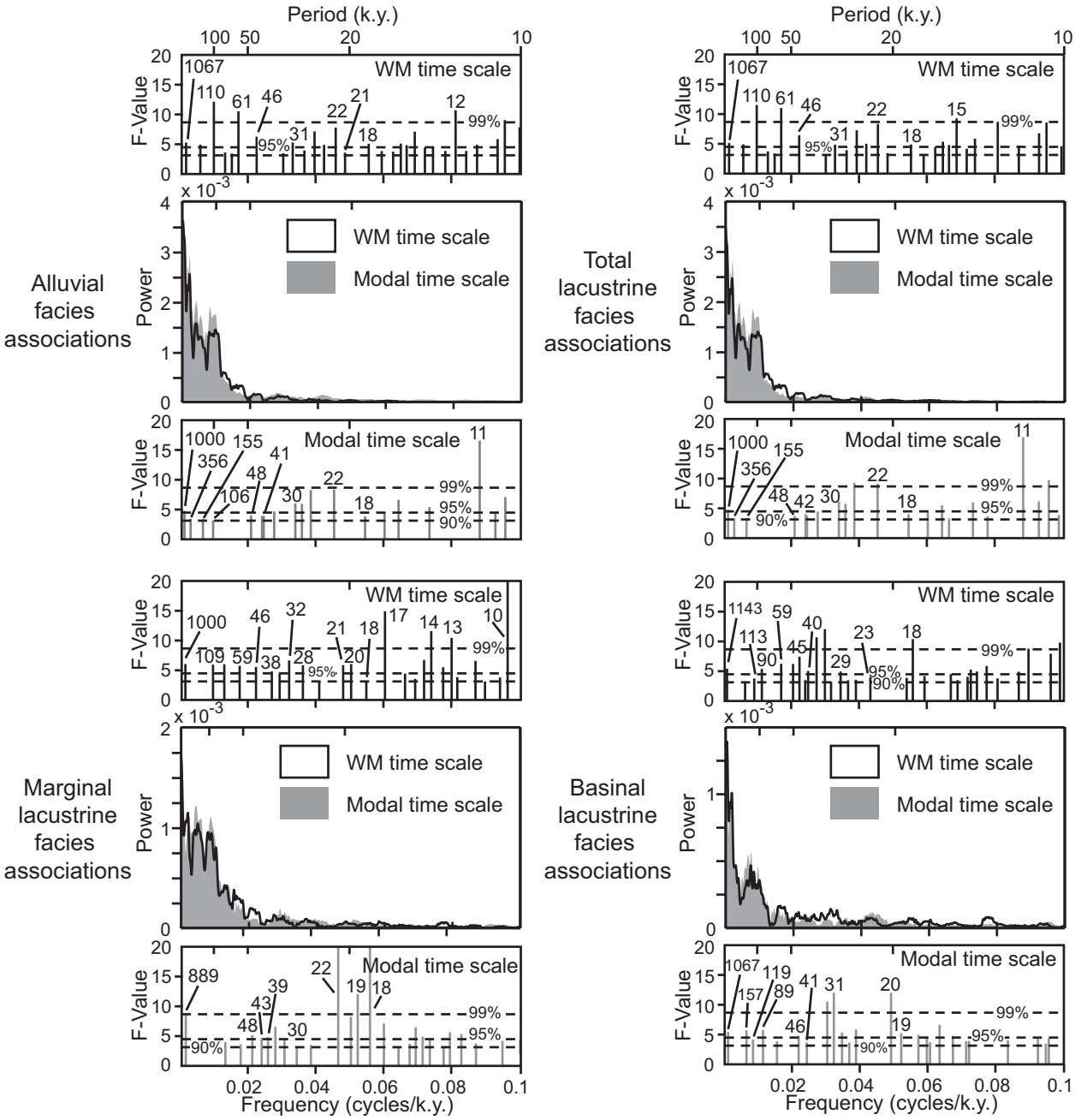

Figure 9. Multitaper method power spectra and F-values of the stratigraphic abundance of each Wilkins Peak facies association, using both the WM and modal time scales. Analyses are conducted with five 3π data tapers, following the removal of a linear trend. The frequency axes are identical for all graphs, and results are plotted from a frequency of 5.5 × 10^{-4} to 0.1 cycles/k.y. (high power at frequencies < 5.5 × 10^{-4} is excluded to aid in illustration). Dashed lines indicate 90%, 95%, and 99% levels of confidence for the harmonic F-test for the presence of periodic components. F-values below the 90% confidence level are excluded from the plot. Note that although not displayed, an F-value achieving the 89.89% confidence level is present at ~1/106 k.y. for the modal time scale total lacustrine facies association.

sensitivity is expected, since Fourier spectral estimates are inherently more sensitive at higher frequencies, and thus short-term inaccuracies in the time scale will appear more substantial. Numerous periods with significant F-values occur within the sub–100 k.y. range, some of which appear to match expected obliquity and precessional modes. In contrast to the alluvial and the total lacustrine facies associations, the marginal lacustrine and the basinal lacustrine results demonstrate a larger fraction of their variance at frequencies between 1/10 k.y. and 1/100 k.y.

At very low frequencies, an ~400 k.y. cycle of high power is apparent, consistent with long eccentricity as hypothesized in previous studies (Meyers, 2008; Machlus et al., 2008). The modal time scale alluvial and total lacustrine spectra are the only results for which this cycle exceeds the 90% F-test confidence level. All facies associations based on both time scales also resolve a previously poorly documented low-

TABLE 1. THEORETICAL AND OBSERVED PERIODS FOR THE EOCENE WILKINS PEAK MEMBER MACROSTRATIGRAPHIC DATA SERIES

	Alluvial facies association		Total lacustrine facies association		Marginal lacustrine facies association		Basinal lacustrine facies association	
Predicted orbital periods (k.y.)	Observed periods (k.y.)	MTM probability (%)	Observed periods (k.y.)	MTM probability (%)	Observed periods (k.y.)	MTM probability (%)	Observed periods (k.y.)	MTM probability (%)
WM time scale								
400.00	N.A.*	N.A.	N.A.	N.A.	N.A.	N.A.	N.A.	N.A.
130.23	109.59	99.62	109.59	99.55	108.84	97.40	112.68	92.86
97.94							89.89	96.67
50.76	45.98	97.67	46.11	97.84	45.71	96.96	49.23	97.63
39.14					37.65	95.79	40.40	96.12
21.83	22.19	98.66	22.22	98.89	21.00	97.31	23.22	93.90
18.74	18.24	96.14	18.24	95.90	20.00	97.50	18.60	93.25
Modal time scale								
400.00	355.56	91.55	355.56	90.82	N.A.	N.A.	N.A.	N.A.
130.23	105.96	90.04	105.96	89.89†	N.A.	N.A.	120.30	94.33
97.94					N.A.	N.A.	88.89	97.19
50.76	48.48	93.66	48.48	92.62	48.19	96.41	45.98	95.78
39.14	41.03	93.34	41.13	92.74	39.41	95.84	41.34	92.75
21.83	22.16	98.89	22.16	99.11	21.68	99.94	20.41	99.61
18.74	18.43	93.01	18.43	93.72	19.28	99.62	19.23	96.53

Note: Observed periods were calculated using the multitaper method (MTM). Predicted orbital periods were derived from orbital solutions La2004 (obliquity and precession; Laskar et al., 2004) and La2010 (eccentricity; Laskar et al., 2011).

*N.A. indicates that none of the observed significant periods (90% confidence level) is close to predicted orbital periods.

†Although not exceeding 90% confidence level, the 105.96 k.y. period of the total lacustrine facies association is shown because it is very consistent with that of the alluvial association.

frequency component at a period of ~1000 k.y., which could be a modulator of obliquity (Laskar et al., 20004; Machlus et al., 2008). Although this period has very high power, the length of the time series (~1700 k.y.) prohibits more rigorous assessment of this potential cycle.

DISCUSSION

The 100 k.y. Cycle

The strong ~100 k.y. cyclicity found in this study is in good general agreement with results from previous studies that were based solely on Fischer assay data from individual cores (Meyers, 2008; Machlus et al., 2008). More specifically, the ~109 k.y. period seen in the alluvial, total lacustrine, and marginal lacustrine spectra of the WM time scale and the ~106 k.y period seen in the alluvial and total lacustrine spectra of the modal time scale (Table 1; Fig. 9) are close matches to the 105 k.y. tuning frequency assumed by Machlus et al. (2008). The agreement is remarkable, considering that the present analyses do not employ orbital tuning, but instead rely exclusively on radioisotopic tuff ages for calibration. These results agree less closely with Machlus et al.'s (2008) second model, which involved tuning the Fischer assay oil yield at two sites individually to precessional cycles (Roehler, 1993) and resolved ~102 k.y. and ~98 k.y. periods. The average spectral misfit between a single core and predicted orbital periods also estimated the co-occurrence of two periods of ~120 k.y. and ~95 k.y. (~108 k.y. on average) by assuming constant net accumulation rates throughout the deposition of the Wilkins Peak Member (Meyers, 2008). The fact that three studies using entirely different analytical approaches produced similar results confirms that an ~100 k.y. cycle is indeed a strong intrinsic feature of the Wilkins Peak Member.

Evaluation of Orbital Forcing in the Wilkins Peak Member: Proxy and Method Challenges

Previous studies of Wilkins Peak Member cyclicity have generally concluded that orbital forcing is expressed in the rhythmic succession of its carbonate-rich lacustrine facies, which in turn reflects expansion and contraction of Eocene Lake Gosiute (Fischer and Roberts, 1991; Roehler, 1993; Meyers, 2008; Machlus et al., 2008). However, a limitation of those studies is that they relied on Fischer assay data to serve as a faithful proxy for lake depth, rather than on actual facies descriptions. Fischer Assay data do bring some specific advantages; the data are plentiful and free, due to extensive past oil shale resource surveys conducted by the U.S. Bureau of Mines, and they avoid the potential for subjectivity that can occur with visual facies description. Moreover, increased organic enrichment does appear to correlate with visual facies evidence for deep lacustrine deposition (e.g., Carroll and Bohacs, 2001; Pietras and Carroll, 2006). Nevertheless, Fischer assay analyses do not represent truly continuous time series, because they represent samples that are homogenized across discrete core intervals. These intervals typically range from 1 to 5 ft (0.3–1.5 m) in thickness, which limits their temporal resolution (Pietras et al., 2003; Pietras and Carroll, 2006). The most significant disadvantage of Fischer assay data is that they convey no direct information about rocks that lack significant organic matter, such as the siliciclastic alluvial intervals and evaporite beds. The role that these intervals may have played in preserving a record of orbital forcing of sedimentation was therefore not directly evaluated in any of the previous studies based on Fischer assay data. However, the importance of the alluvial intervals could be implied from the observation that ~100 k.y. periodicity is most strongly expressed at localities where the alluvial intervals are most prominent (Machlus et al., 2008).

The first proposal that the nine discrete Wilkins Peak alluvial intervals record climatic forcing related to short eccentricity was based on direct interpolation between radioisotopic ages ($^{40}Ar/^{39}Ar$ and U-Pb) of intercalated tuffs (Smith et al., 2010). They further proposed calibration of the alluvial intervals directly to specific predicted minima in long and short eccentricity (Laskar et al., 2004). This calibration remains uncertain, however, due to errors that could result both from interpolating average sediment accumulation rates and from extrapolating the astronomical solutions back to the Eocene. Their study was also limited to a single drill core, whereas preservation of the nine alluvial siliciclastic intervals is variable across the Bridger Basin. The number of alluvial intervals generally decreases going northward, and at some locations only the "D" interval can be identified (Fig. 2).

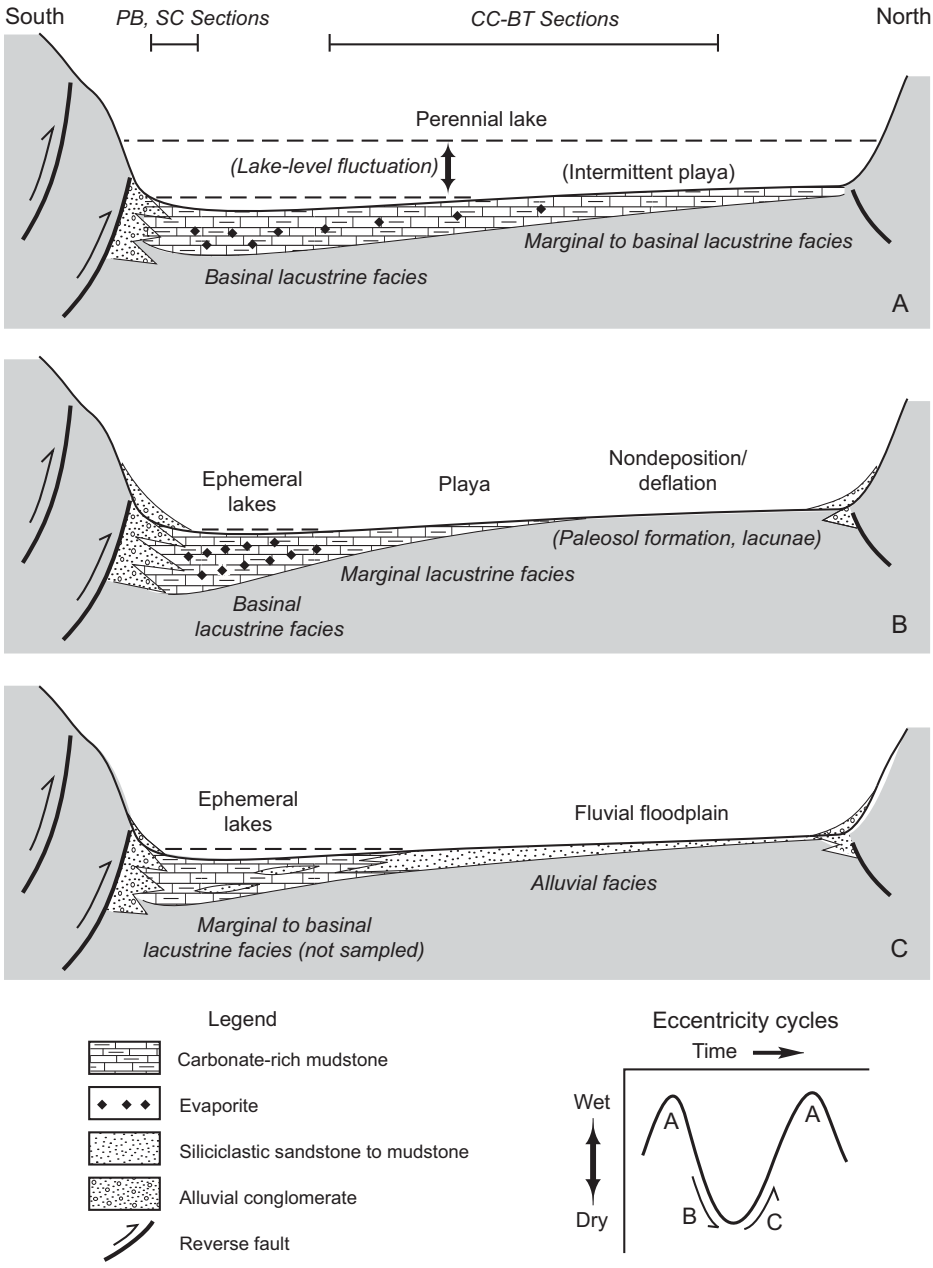

Figure 10. Conceptual model for the origin of alternating lacustrine versus alluvial facies associations in the Wilkins Peak Member (not to scale). Higher-frequency lake-level fluctuations are omitted for clarity. Bars at top indicate the approximate basin positions of the stratigraphic sections utilized in this study (Figs. 1 and 2). (A) All study locations are inundated by Lake Gosiute. The lacustrine facies associations are widely distributed during this stage, whereas deposition of fine-grained siliciclastic alluvial sediments is prohibited. (B) Lake Gosiute is in a contraction stage. The lake floor is generally exposed, with ephemeral lakes. Deposition occurs only in the deepest part of the basin, where evaporite forms. (C) Fine-grained siliciclastic alluvial sediments are deposited as the lake begins to expand. Evaporite deposition is interrupted. Later, deposition of the lacustrine facies associations overwhelms the alluvial deposition (A).

A Depositional Model for 100 k.y. Cycle Expression in the Wilkins Peak Member

Macrostratigraphy reveals that eccentricity cycles are not primarily recorded in the Wilkins Peak Member through fluctuations of Lake Gosiute water level, represented by the rhythmic successions of lacustrine strata, but instead by the alternation of siliciclastic alluvial and carbonate-rich lacustrine strata (Figs. 8 and 9). This realization has considerable practical significance, because the specific alluvial intervals (A through I) are readily identifiable in outcrop, providing a useful in situ chronometer.

The extensive alluvial intervals clearly record the activity of river systems that crossed the basin (Pietras and Carroll, 2006; Williams and Carroll, 2009), most likely originating to the northeast of the basin (Smoot, 1983; Sullivan, 1985). Their very existence within a closed basin might be seen as paradoxical, because active river systems imply a positive hydrologic budget that would also be expected to cause lake expansion (Bohacs et al., 2000). However, detailed sedimentologic study of the siliciclastic intervals instead supports a purely fluvial origin as a well-channelized fluvial depositional environment dominated by accreting macroforms (Williams and Carroll, 2009). Incipient paleosol formation is also evident in lake-plain facies immediately underlying at least one alluvial interval (Pietras and Carroll, 2006). Such exposure surfaces are hypothesized to have formed during exceptionally dry periods when the lake had shrunken or disappeared entirely (Fig. 10B), and then fluvial deposition commenced as conditions initially became wetter again (Fig. 10C). Finally, the alluvial deposits were inundated by Lake Gosiute (Fig. 10A). The bimodal hypsometry of the basin, which consisted of a low-gradient floor surrounded by much steeper bedrock exposures (Pietras and Carroll, 2006), may also have contributed to the strong contrast and rapid transition between siliciclastic and carbonate facies. Once Lake Gosiute dropped below the level of its bedrock boundaries, any further small decrease in water depth would have caused it to very rapidly shrink or disappear, exposing the lake plain to fluvial influence. The same low-gradient basin floor would promote rapid re-flooding of the basin.

High-Frequency Variability

When compared to the other facies associations, the marginal lacustrine and basinal lacustrine power spectra reveal a larger fraction of their variance at frequencies between 1/10 k.y. and 1/100 k.y. (Fig. 9). The high-frequency alternation between basinal and marginal associations—including the power in the obliquity and precession bands—is postulated to be the result of fluctuations in lake level (Figs. 8 and 9). This interpretation is supported by the lack of substantial high-frequency variation in the combined lacustrine association, indicating that the two components are consistently out phase

with each other, as would be expected if the lake-level changes were generally synchronous across the basin (Fig. 8). In contrast, the high-power ~1/100 k.y. cycle observed in these facies associations is largely attributable to the diminishment of lacustrine facies at times of extensive alluvial deposition (A through I) as observed in the macrostratigraphic time series.

The power spectra obtained from macrostratigraphic time series differ in fine detail from those reported by Meyers (2008) and Machlus et al. (2008), but they share feature with those studies—a general multiplicity of low-power spectral peaks at higher frequencies (periods shorter than 100 k.y.)—far more than expected by the orbital hypothesis. There are a variety of possible explanations for the "noisy" nature of the high-frequency portions of the spectra, including non-Milankovitch forcing such as stochastic geomorphic processes that affected lake level (e.g., autocyclicity), strongly nonlinear responses of the climate and/or the depositional system to orbital-insolation forcing, taphonomic artifacts associated with the depositional system, or spectral artifacts related to the nature of the input data or the methodologies used to estimate spectra. With respect to the first explanation, there exists a robust physical record of subprecessional lake-level fluctuation (Pietras et al., 2003). Based on tuff ages (Smith et al., 2003) and on lake cycles described in outcrops and cores, that study reported average cycle durations as short as 10 k.y. for the Wilkins Peak Member in the WM core (Fig. 1). Moreover, the thinnest complete lake cycles could be shorter (Pietras and Carroll, 2006). Neither of those studies claimed to exclude the existence of lake cycles influenced by precessional or longer variability, but no definitive sedimentologic or stratigraphic criteria presently exist for distinguishing cycles that result from orbital forcing versus those that reflect other controls on lake level.

On the basis of a general circulation model used to study mechanisms for translating the orbital signal into climatologic, geomorphic, and sedimentologic processes, precessional forcing of lake levels in Eocene Lake Gosiute is plausible (Morrill et al., 2001). Such forcing would likely have been expressed as changing rates of evaporation from the lake surface, related to changing shortwave radiation, rather than by changes in mean annual precipitation. They also noted that additional local factors could complicate the response of lake level to orbital-insolation variability, including changes in vegetation, mud-flat area surrounding the lake, snowmelt variability, and changes in catchment.

Rather than infer weak orbital forcing of Eocene climate based on high-frequency variability, the lacustrine facies associations of the Wilkins Peak Member are instead hypothesized to constitute an intrinsically noisy system that has distorted the apparent orbital insolation signal through a taphonomic filter. Such taphonomic influences likely include unresolved changes in sedimentation rate (Meyers et al., 2001), which tend to smear high-frequency components in power spectra (known as "peak splitting"). Furthermore, variable sedimentation within individual "cycles" can introduce artifacts that resemble harmonics of the fundamental cycle (e.g., 1/2, 1/3, and 1/4 of the precession period), a mathematical consequence of the departure of the sedimentary rhythm from a purely sinusoidal shape (Schiffelbein and Dorman, 1986). Bioturbational mixing is another important taphonomic filter that can dampen the expression of high-frequency variability (Goreau, 1980; Ripepe and Fischer, 1991), as well as other processes associated with sediment delivery, deposition, and burial (e.g., Ripepe and Fischer, 1991; Meyers and Sageman, 2004; Laurin et al., 2005; Jerolmack and Paola, 2010).

Macrostratigraphy as a Tool for Cyclostratigraphic Study

Macrostratigraphy helps to overcome many of the difficulties noted here by synthesizing observations from multiple localities. It also allows the spectral contributions of individual facies associations to be assessed separately. This in turn makes it possible to more deeply examine the way in which the expression of an expected climatic forcing signal is related to the detailed geomorphic and depositional processes that are responsible for recording it. These sedimentary "transfer functions" (Meyers et al., 2008) are fundamentally important both for understanding the past behavior of Earth's climate, and for building a reliable astrochronologic time scale, but they have seldom been critically evaluated.

Another advantage of macrostratigraphy is that it has been empirically demonstrated to be robust to very incomplete spatial sampling (Hannisdal and Peters, 2010). Regarding the specific cores and outcrops employed in the present study, the geometry of the basin suggests that the sampling transect (Fig. 1), which captures a large fraction of the depositional environments (Fig. 10), should be sufficient to quantify basin-scale depositional patterns. This is due to the fact that siliciclastic sediments are supplied from an extrabasinal point source to the northeast, and then redistributed throughout the closed basin. While different transects could result in either dampening or amplification of signals, the extensive transect employed here (Figs. 1 and 10) is unlikely to fail to capture the depositional forcing mechanisms recorded in the repetitive sedimentary successions of the Wilkins Peak Member. In other words, it is unlikely that any large-scale signals preserved in this geologic record are missed by the macrostratigraphic quantification.

CONCLUSIONS

Wilkins Peak stratigraphy, based on a detailed regional cross section of 12 high-resolution stratigraphic sections, geochronology, macrostratigraphy, and spectral analysis, advances fundamental understanding of the complex mechanisms responsible for generating the repetitive stratigraphic succession of the Wilkins Peak Member. Although macrostratigraphy displays some sensitivity to the time model used for the thickness-to-time transformation, its efficacy in the incorporation of temporal and spatial variability of geologic records provides an outstanding quantitative framework for basin-scale analysis. It allows us to better constrain the complex links between orbital forcing and sedimentation in the Wilkins Peak Member.

The macrostratigraphic time series indicate a strongly reciprocal relationship between carbonate-rich lacustrine facies and siliciclastic alluvial facies. Multitaper method spectral analyses of the macrostratigraphic data resolve significant periods (≥90% confidence level by F-test) that are consistent with the predicted orbital periods, with a particularly strong ~100 k.y. cycle. Depositional controls on the alluvial bed sets are interpreted to be strongly influenced by short-eccentricity variability, and have a pronounced impact on the Wilkins Peak depositional cyclicity. Consequently, the alternation between siliciclastic alluvial sedimentation and carbonate-rich lacustrine sedimentation is proposed to be responsible for recording eccentricity cycles in the Wilkins Peak Member. This is in contrast to simple lake-level fluctuations, which had a strong impact on lacustrine deposition only on a shorter time scale. Numerous non-Milankovitch periods were also identified, implying nonlinear responses to the orbital forcing, substantial taphonomic distortion, and/or the potential for high-frequency autocyclic processes. Further examination of the differences amongst the spectral results from the different facies associations should yield insight into the transfer functions associated with the depositional system, ranging from proximal to distal settings, and therefore, a quantitative assessment of both orbitally and nonorbitally influenced depositional processes that serve to amplify, diminish, and distort the primary orbital-insolation signal.

ACKNOWLEDGMENTS

J.T. Pietras is greatly thanked for providing the detailed Wilkins Peak stratigraphy of the northern part of the Bridger Basin. Other individuals contributed

helpful discussions or other assistance, including K.M. Bohacs, A.E. Carlson, C.S. Clay, R.H. Dott, J.R. Dyni, A.G. Fischer, L.A. Hinnov, D.C. Kelly, T.K. Lowenstein, M.L. Machlus, G.M. Mason, J.P. Smoot, and E.M. Williams. Green River Formation research at the University of Wisconsin–Madison was funded by National Science Foundation grants EAR-0230123, EAR-0114055, and EAR-0516760, Conoco-Phillips, Chevron-Texaco, the Donors to the Petroleum Research Fund of the American Chemical Society, the Center for Oil Shale Technology and Research, and the Department of Geoscience, University of Wisconsin. Chronology development and time-series analyses were supported by National Science Foundation grant OCE-1003603 to S. Meyers. Field work was supported by the Geological Society of America.

REFERENCES CITED

Bohacs, K.M., 1998, Contrasting expressions of depositional sequences in mudrocks from marine to nonmarine environs, *in* Schieber, J., Zimmerle, W., and Sethi, P., eds., Shales and Mudstones I: Stuttgart, Germany, Schweizerbart'sche Verlagsbuchhandlung, p. 33–78.

Bohacs, K.M., Carroll, A.R., Neal, J.E., and Mankiewicz, P.J., 2000, Lake-basin type, source potential, and hydrocarbon character: An integrated sequence-stratigraphic geochemical framework, *in* Gierlowski-Kordesch, E.H., and Kelts, K.R., eds., Lake Basins through Space and Time: American Association of Petroleum Geologists Studies in Geology 46, p. 3–34.

Bradley, W.H., 1929, The Varves and Climate of the Green River Epoch: U.S. Geological Survey Professional Paper 158-E, 110 p.

Bradley, W.H., and Eugster, H.P., 1969, Geochemistry and Paleolimnology of the Trona Deposits and Associated Authigenic Minerals of the Green River Formation of Wyoming: U.S. Geological Survey Professional Paper 496-B, 71 p.

Carroll, A.R., and Bohacs, K.M., 1999, Stratigraphic classification of ancient lakes: Balancing tectonic and climatic controls: Geology, v. 27, p. 99–102, doi:10.1130/0091-7613(1999)027<0099:SCOALB>2.3.CO;2.

Carroll, A.R., and Bohacs, K.M., 2001, Lake-type controls on petroleum source rock potential in nonmarine basins: The American Association of Petroleum Geologists Bulletin, v. 85, p. 1033–1053.

Culbertson, W.C., 1961, Stratigraphy of the Wilkins Peak Member of the Green River Formation, Firehole Basin Quadrangle, Wyoming: U.S. Geological Survey Professional Paper 424D, p. 170–173.

Fischer, A.G., and Roberts, L.T., 1991, Cyclicity in the Green River Formation (lacustrine Eocene) of Wyoming: Journal of Sedimentary Petrology, v. 61, p. 1146–1154.

Goreau, T.J., 1980, Frequency sensitivity of the deep-sea climatic record: Nature, v. 287, p. 620–622, doi:10.1038/287620a0.

Hannisdal, B., and Peters, S.E., 2010, On the relationship between macrostratigraphy and geological processes: Quantitative information capture and sampling robustness: Journal of Geology, v, 118, p. 111–130.

Hinnov, L.A., and Ogg, J.G., 2007, Cyclostratigraphy and the astronomical time scale: Stratigraphy, v. 4, p. 239–251.

Huybers, P., and Wunsch, C., 2004, A depth-derived Pleistocene age model: Uncertainty estimates, sedimentation variability, and nonlinear climate change: Paleoceanography, v. 19, PA1028, 24 p.

Jerolmack, D.J., and Paola, C., 2010, Shredding of environmental signals by sediment transport: Geophysical Research Letters, v. 37, L19401, 5 p.

Kuiper, K.F., Deino, A., Hilgen, F.J., Krijgsman, W., Renne, P.R., and Wijbrans, J.R., 2008, Synchronizing rock clocks of Earth history: Science, v. 320, p. 500–504, doi:10.1126/science.1154339.

Laskar, J., Robutel, P., Joutel, F., Gastineau, M., Correia, A.C.M., and Levrard, B., 2004, A long-term numerical solution for the insolation quantities of the Earth: Astronomy & Astrophysics, v. 428, p. 261–285, doi:10.1051/0004-6361:20041335.

Laskar, J., Fienga, A., Gastineau, M., and Manche, H., 2011, La2010: A new orbital solution for the long-term motion of the Earth: Astronomy and Astrophysics, v. 532, no. A89, 15 p.

Laurin, J., Meyers, S.R., Sageman, B.B., and Waltham, D., 2005, Phase-lagged amplitude modulation of hemipelagic cycles: A potential tool for recognition and analysis of sea-level change: Geology, v. 33, p. 569–572, doi:10.1130/G21350.1.

Machlus, M.L., Olsen, P.E., Christie-Blick, N., and Hemming, S.R., 2008, Spectral analysis of the lower Eocene Wilkins Peak Member, Green River Formation, Wyoming: Support for Milankovitch cyclicity: Earth and Planetary Science Letters, v. 268, p. 64–75, doi:10.1016/j.epsl.2007.12.024.

Meyers, S.R., 2008, Resolving Milankovitchian controversies: The Triassic Latemar Limestone and the Eocene Green River Formation: Geology, v. 36, p. 319–322, doi:10.1130/G24423A.1.

Meyers, S.R., and Sageman, B.B., 2004, Detection, quantification, and significance of hiatuses in pelagic and hemipelagic strata: Earth and Planetary Science Letters, v. 224, p. 55–72, doi:10.1016/j.epsl.2004.05.003.

Meyers, S.R., and Sageman, B.B., 2007, Quantification of deep-time orbital forcing by average spectral misfit: American Journal of Science, v. 307, p. 773–792, doi:10.2475/05.2007.01.

Meyers, S.R., Sageman, B., and Hinnov, L., 2001, Integrated quantitative stratigraphy of the Cenomanian-Turonian Bridge Creek Limestone Member using evolutive harmonic analysis and stratigraphic modeling: Journal of Sedimentary Research, v. 71, p. 628–644, doi:10.1306/012401710628.

Meyers, S.R., Sageman, B.B., and Pagani, M., 2008, Resolving Milankovitch: Consideration of signal and noise: American Journal of Science, v. 308, p. 770–786, doi:10.2475/06.2008.02.

Morrill, C., Small, E.E., and Sloan, L.C., 2001, Modeling orbital forcing of lake level change: Lake Gosiute (Eocene): North America: Global and Planetary Change, v. 29, p. 57–76, doi:10.1016/S0921-8181(00)00084-9.

Muller, R.A., and MacDonald, G.J., 2000, Ice Ages and Astronomical Causes: Data, Spectral Analysis and Mechanisms: London, Springer, 318 p.

Pestiaux, P., and Berger, A., 1984, Impacts of deep-sea processes on paleoclimate spectra, *in* Berger, A., Imbrie, J., Hays, J., Kukla, G., and Saltzman, B., eds., Milankovitch and Climate, Part 1: Boston, D. Reidel Publishing Company, p. 493–510.

Peters, S.E., 2006, Macrostratigraphy of North America: The Journal of Geology, v. 114, p. 391–412, doi:10.1086/504176.

Pietras, J.T., and Carroll, A.R., 2006, High-resolution stratigraphy of an underfilled lake basin: Wilkins Peak Member, Eocene Green River Formation, Wyoming, U.S.A.: Journal of Sedimentary Research, v. 76, p. 1197–1214, doi:10.2110/jsr.2006.096.

Pietras, J.T., Carroll, A.R., Singer, B.S., and Smith, M.E., 2003, 10 k.y. depositional cyclicity in the early Eocene: Stratigraphic and $^{40}Ar/^{39}Ar$ evidence from the lacustrine Green River Formation: Geology, v. 31, p. 593–596, doi:10.1130/0091-7613(2003)031<0593:KDCITE>2.0.CO;2.

Prokoph, A., Villeneuve, M., Agterberg, F.P., and Rachold, V., 2001, Geochronology and calibration of global Milankovitch cyclicity at the Cenomanian-Turonian boundary: Geology, v. 29, p. 523–526, doi:10.1130/0091-7613(2001)029<0523:GACOGM>2.0.CO;2.

Ripepe, M., and Fischer, A.G., 1991, Stratigraphic rhythms synthesized from orbital variations, *in* Franseen, E.K., Watney, W.L., Kendall, C.G.St.C., and Ross, W., eds., Sedimentary Modeling: Computer Simulations and Methods for Improved Parameter Definition: Kansas State Geological Survey Bulletin 233, p. 335–344.

Roehler, H.W., 1993, Eocene Climates, Depositional Environments, and Geography, Greater Green River Basin, Wyoming, Utah, and Colorado: U.S. Geological Survey Professional Paper 1506F, 74 p.

Schiffelbein, P., and Dorman, L., 1986, Spectral effects of time-depth nonlinearities in deep sea sediment records: A demodulation technique for realigning time and depth scales: Journal of Geophysical Research, v. 91, p. 3821–3835, doi:10.1029/JB091iB03p03821.

Silverman, B.W., 1982, Algorithm AS 176: Kernel density estimation using the fast Fourier transform: Journal of the Royal Statistical Society, ser. C, Applied Statistics, v. 31, p. 93–99.

Sloan, L.C., and Rea, D.K., 1996, Atmospheric carbon dioxide and early Eocene climate: A general circulation modeling sensitivity study: Palaeogeography, Palaeoclimatology, Palaeoecology, v. 119, p. 275–292, doi:10.1016/0031-0182(95)00012-7.

Smith, M.E., 2007, Stratigraphy, Geochronology, and Paleogeography of the Green River Formation, Wyoming, Colorado, and Utah [Ph.D. thesis]: Madison, Wisconsin, University of Wisconsin, 318 p.

Smith, M.E., Singer, B.S., and Carroll, A.R., 2003, $^{40}Ar/^{39}Ar$ geochronology of the Eocene Green River Formation, Wyoming: Geological Society of America Bulletin, v. 115, p. 549–565, doi:10.1130/0016-7606(2003)115<0549:AGOTEG>2.0.CO;2.

Smith, M.E., Carroll, A.R., and Singer, B.S., 2008, Synoptic reconstruction of a major ancient lake system: Eocene Green River Formation, western United States: Geological Society of America Bulletin, v. 120, p. 54–84, doi:10.1130/B26073.1.

Smith, M.E., Chamberlain, K.R., Singer, B.S., and Carroll, A.R., 2010, Eocene clocks agree: Coeval $^{40}Ar/^{39}Ar$, U-Pb, and astronomical ages from the Green River Formation: Geology, v. 38, p. 527–530, doi:10.1130/G30630.1.

Smoot, J.P., 1983, Depositional subenvironments in an arid closed basin: Wilkins Peak Member of the Green River Formation (Eocene), Wyoming, U.S.A.: Sedimentology, v. 30, p. 801–827, doi:10.1111/j.1365-3091.1983.tb00712.x.

Sullivan, R., 1985, Origin of lacustrine rocks of the Wilkins Peak Member, Wyoming: The American Association of Petroleum Geologists Bulletin, v. 69, p. 913–922.

Thomson, D.J., 1982, Spectrum estimation and harmonic analysis: Proceedings of the Institute of Electrical and Electronics Engineers, v. 70, p. 1055–1096.

Thomson, D.J., 1990, Quadratic-inverse spectrum estimates: Applications to paleoclimatology: Philosophical Transactions of the Royal Society of London, ser. A, Mathematical and Physical Sciences, v. 332, p. 539–597, doi:10.1098/rsta.1990.0130.

Wheeler, H.E., 1958, Time-stratigraphy: Bulletin of the American Association of Petroleum Geologists, v. 42, p. 1047–1063.

Wiig, S.V., Grundy, W.D., and Dyni, J.R., 1995, Trona Resources in the Green River Basin, Southwest Wyoming: U.S. Geological Survey Open-File Report 95-476, 88 p.

Wilf, P., 2000, Late Paleocene–early Eocene climate changes in southwestern Wyoming: Paleobotanical analysis: Geological Society of America Bulletin, v. 112, p. 292–307, doi:10.1130/0016-7606(2000)112<292:LPECCI>2.0.CO;2.

Williams, E.M., and Carroll, A.R., 2009, Depositional environments of clastic-dominated intervals of the Wilkins Peak Member (Eocene), Green River Formation, southwest Wyoming: Geological Society of America Abstracts with Programs, v. 41, no. 7, p. 511.

Zachos, J.C., Stott, L.D., and Lohmann, K.C., 1994, Evolution of early Cenozoic marine temperatures: Paleoceanography, v. 9, p. 353–387, doi:10.1029/93PA03266.

Zachos, J.C., Pagani, M., Sloan, L., Thomas, E., and Billups, K., 2001, Trends, rhythms, and aberrations in global climate 65 Ma to present: Science, v. 292, p. 686–693, doi:10.1126/science.1059412.

Science Editor: A. Hope Jahren
Associate Editor: Brian R. Pratt; Stephen C. Ruppel

Manuscript Received 10 May 2011
Revised Manuscript Received 20 April 2012
Manuscript Accepted 30 April 2012

Printed in the USA